U.S. Department of Veterans Affairs
Public Access Author manuscript
Bone. Author manuscript; available in PMC 2022 February 01.

Published in final edited form as:
Bone. 2021 February ; 143: 115632. doi:10.1016/j.bone.2020.115632.

Reversing cortical porosity: Cortical pore infilling in preclinical models of chronic kidney disease

Corinne E. Metzger[1,*], **Elizabeth A. Swallow**[1,*], **Alexander J. Stacy**[1], **Samantha P. Tippen**[1], **Max A. Hammond**[1], **Neal X. Chen**[2], **Sharon M. Moe**[1,2,4], **Matthew R. Allen**[1,2,3,4]

[1]Department of Anatomy, Cell Biology, Physiology, Indiana University School of Medicine, Indianapolis IN, United States

[2]Department of Medicine – Division of Nephrology, Indiana University School of Medicine, Indianapolis IN, United States

[3]Department of Biomedical Engineering, Indiana University Purdue University of Indianapolis, Indianapolis, IN, United States

[4]Roudebush Veterans Administration Medical Center, Indianapolis, IN, United States

Abstract

Purpose: Chronic kidney disease (CKD) patients have a high incidence of fracture due in part to cortical porosity. The goal of this study was to study cortical pore infilling utilizing two rodent models of progressive CKD.

Methods: Exp 1: Female C57BI/6J mice (16-week-old) were given dietary adenine (0.2%) to induce CKD for 10 weeks after which calcium water supplementation ($Ca\text{-}H_2O$; 1.5% and 3%) was given to suppress PTH for another 4 weeks. Exp 2: Male Cy/+ rats were aged to ~30 weeks with baseline porosity assessed using *in vivo* μCT. A second *in vivo* scan followed 5-weeks of $Ca\text{-}H_2O$ (3%) supplementation.

Results: Exp 1: Untreated adenine mice had elevated blood urea nitrogen (BUN), parathyroid hormone (PTH), and cortical porosity (~2.6% porosity) while $Ca\text{-}H_2O$ lowered PTH and cortical porosity (0.5-0.8% porosity). Exp 2: Male Cy/+ rats at baseline had variable porosity (0.5% - 10%), but after PTH suppression via $Ca\text{-}H_2O$, cortical porosity in all rats was lower than 0.5%.

Send Correspondence to: Matthew R. Allen, PhD, Dept. of Anatomy, Cell Biology, Physiology, MS 5035, Indiana University School of Medicine, 635 Barnhill Dr., Indianapolis, IN 46202, matallen@iu.edu.
*Co-First Authors

Credit author statement
Corinne E. Metzger, Conceptualization, Investigation, Writing - Original Draft, Writing - Review & Editing, Funding acquisition; Elizabeth A. Swallow, Conceptualization, Investigation, Writing - Original Draft, Writing - Review & Editing; Alexander J. Stacy, Investigation; Samantha P. Tippen, Investigation; Max A. Hammond, Software, Formal analysis; Neal X. Chen, Investigation, Resources; Sharon M. Moe, Conceptualization, Resources, Supervision, Funding acquisition; Matthew R. Allen, Conceptualization, Writing - Review & Editing, Funding acquisition

Corinne Metzger, Elizabeth Swallow, Alexander Stacy, Samantha Tippen, Max Hammond, Neal Chen, Sharon Moe, and Matthew Allen declare that they have no conflicts of interest related to the presented work.

Individual pore dynamics measured via a custom MATLAB code demonstrated that 85% of pores infilled while 12% contracted in size.

Conclusion: Ca-H_2O supplementation causes net cortical pore infilling over time and imparted mechanical benefits. While calcium supplementation is not a viable clinical treatment for CKD, these data demonstrate pore infilling is possible and further research is required to examine clinically relevant therapeutics that may cause net pore infilling in CKD.

Keywords

Chronic kidney disease (CKD); Bone; Cortical Porosity

INTRODUCTION

Skeletal fragility in chronic kidney disease (CKD) is common. End-stage renal disease (ESRD) patients have a 4-fold increased risk of fracture compared to their age matched non-CKD counterparts [1]. Fractures in CKD patients not only contribute to reduced mobility and quality of life, but fractures are also associated with a significantly greater rate of mortality in CKD patients compared to patients with normal kidney function [2] [3] [4] [5] [6] [7]. With one in seven people in the United States estimated to have some degree of CKD, preventing or reversing skeletal fragility in CKD would have significant public benefit [2] [8].

As the disease progresses, CKD patients often develop a triad of clinical manifestations known as chronic kidney disease mineral bone disorder (CKD-MBD) including biochemical abnormalities, vascular calcifications, and bone deterioration [9] [10] [11]. Unlike other forms of bone loss which primarily impact trabecular bone, bone deterioration in CKD predominately affects the cortical compartment of bone in the form of cortical porosity. Since cortical bone is important for the mechanical and structural integrity of bone, cortical porosity contributes significantly to increased fractures seen in CKD patients [12] [13]. Reducing cortical porosity may be key in preventing skeletal fragility and improving bone health in CKD patients.

Reduction of cortical porosity can occur through several mechanisms including suppressing new pore formation, suppressing of pore growth, or infilling of pores with a combination likely having greatest benefit on overall porosity. Previous work in animal studies has demonstrated that prevention of cortical pores is possible through suppression of PTH via calcium water supplementation (Ca-H_2O) [14] [15]. It remains largely unknown whether cortical pore infilling is possible and, if so, what conditions are ideal to promote infilling. We aimed to explore this question with two animal models of CKD: 1) adenine-induced CKD in mice and 2) the Cy/+ rat with spontaneous development of polycystic kidney disease. Both models develop characteristics of clinical CKD with impaired kidney function as well as high circulating PTH and cortical porosity [16] [17] [15]. Previously, we have demonstrated that Ca-H_2O is a suppressor of PTH and that it prevents the development of cortical pores. In both models in this study, treatment initiation with Ca-H_2O occurred *after* the development of porosity. Importantly, this is in contrast to our previous work which has focused on cortical pore prevention with treatment initiation (Ca-H_2O) in the early stages of

CKD progression prior to the formation of cortical pores [14] [15].We hypothesized that PTH suppression via calcium water supplementation would reduce porosity in female adenine-induced CKD mice and improve mechanical properties of bone. Secondly, utilizing the male Cy+ model, we hypothesized that cortical porosity would decrease after calcium water supplementation and that individual pore tracking would demonstrate pore infilling over time.

METHODS

Experiment 1

Animals: 15-week-old female C57BI/6J mice (Jackson Laboratories, Bar Harbor, ME, USA; JAX #000664; n=96) were group housed 4/cage in an institutionally approved animal facility. After a one-week acclimation, all control mice were put on a purified casein-based diet with an adjusted calcium and phosphorous ratio (0.9% P, 0.6% CA). All adenine-induced CKD mice were put on the same casein-based diet with the addition of 0.2% adenine (Envigo Teklad Diets, Madison, Wl, USA). All treatment and control groups (n=10-12/group) are described in Figure 1a. Previous studies demonstrated that adenine ingestion in mice results in progressive kidney impairment including elevated creatinine, blood urea nitrogen, and parathyroid hormone [18] [19] [20] [21]. After six weeks on the adenine diet, all adenine mice were switched back to the control diet as we and others have demonstrated that an induction period of adenine is sufficient to result in continued elevations in BUN and PTH in rodents [21] [22] [23] [24] [25]. Ten weeks after initiation of diets, a group of control and adenine mice were anesthetized via inhaled vaporized isoflurane and euthanized via thoracotomy and exsanguination. Remaining control and adenine groups were divided into three groups – standard drinking water (Control and Adenine), 1.5% calcium gluconate drinking water (Con+1.5% and Ad+1.5%), and 3% calcium gluconate drinking water (Con+3% and Ad+3%). Calcium water supplementation (Ca-H_2O) was provided continuously for four weeks followed by euthanasia, 14 weeks after diet initiation. Kidney and right femurs were fixed in 10% neutral buffered formalin. Left femurs were frozen in phosphate buffered saline-soaked gauze. All animal procedures were approved by the Indiana University School of Medicine Institutional Animal Care and Use Committee prior to the initiation of any experimental protocols.

Serum biochemistries: Cardiac serum collected at time of euthanasia was used to measure serum blood urea nitrogen (BUN) via colorimetric assay (BioAssay Systems, Hayward, CA, USA). Serum 1-84 parathyroid hormone was measured via ELISA (Immunotopics Quidel, San Diego, CA, USA) with an intra-assay coefficient of variation of 2.4-5.6% and an inter-assay coefficient of variation of 5.5%.

Ex vivo Micro-Computed Tomography of the Femur: Right distal femurs were scanned on a SkyScan 1172 (Bruker, Billerica, MA, USA) with a 0.5 aluminium filter and a 6 μm voxel size. Cortical bone was analyzed in the femur from 5 slices located ~2.5 mm proximal to the most proximal portion of the distal growth plate. Cortical area, cortical thickness, cortical porosity and pore number were assessed from this site. Cortical porosity was determined by assessing total void volume between the periosteal and endosteal

surfaces, presented as a % of overall cortical volume. Pore number was determined as the number of pores per mm^2 of cortical bone.

Ex vivo Micro-Computed Tomography of the Kidney: Fixed kidneys were scanned on a SkyScan 1176 (Bruker, Billerica, MA, USA) with no filter and a 9 μm voxel size. A 0.5 mm region of interest was selected at the middle of the kidney for assessment of crystal volume/kidney volume within the ROI.

Three-point Bending of the Femur: Frozen left whole femurs were scanned on a SkyScan 1176 (Bruker, Billerica, MA, USA) with a 0.5 aluminium filter and 9 μm voxel size for assessment of mid-shaft cortical geometry. The midshaft region was selected by measuring half the length of the full bone from the CT scan. After thawing, samples underwent a three-point-bend test with a bottom span of 6 mm and the central fixture located approximately at the longitudinal mid-point of the femur (Model 500lbs Actuator with R Controller, Test Resources, Shakopee, MN, USA). All samples were tested until failure with the anterior surface in compression. Samples were kept hydrated with PBS and loaded at 2mm/minute to collect force-displacement data. Mechanical outcome parameters were calculated in a custom MATLAB script using the force-displacement data and cortical geometry parameters generated from a single mid-shaft (1/2 total length) slice as previously described [14] [15] [26] [27]. All data collected used standard nomenclature.

Statistical Analyses: Data from 10-week control and adenine mice were compared via a t-test. All data from the 14-week timepoint except for kidney crystals were analyzed as a 2x3 factorial ANOVA (disease-by-calcium water supplementation) and all main effects and interaction effects noted. If the model 2x3 ANOVA was statistically significant ($p<0.05$), an all-groups Duncan post hoc analysis was applied to determine differences between groups. Kidney crystals were analyzed via a one-way ANOVA at the 14-week timepoint between all adenine groups due to the lack of crystals in all control kidneys. All statistical analyses were completed with IBM SPSS Statistics 26 (IBM, Armonk, NY, USA). Data are represented as mean ± standard deviation.

Experiment 2

Animals.—Male Sprague Dawley Cy/+ rats (n=6) were placed on a casein-based diet with adjusted calcium and phosphorous ratio (0.6% and 0.9%, respectively) at 18 weeks of age. *In-vivo* μCT scans were performed for baseline measures of porosity at 30 weeks of age. Previous longitudinal data from our lab has shown that cortical porosity often develops around 30 weeks of age and, in some cases, severe cortical porosity is seen by 35 weeks of age [28]. All animals (n=6) were then provided calcium supplementation via 3% calcium gluconate drinking water ($Ca\text{-}H_20$) for 5 weeks (Figure 1b). In this study our goal was to investigate cortical infilling, therefore, $Ca\text{-}H_2O$ commenced *after* the development of cortical pores [28]. At 35 weeks of age animals underwent a second μCT scan and then were anesthetized via inhaled vaporized isoflurane and euthanized via thoracotomy and exsanguination. All study procedures were approved by the Indiana University School of Medicine Institutional Animal Care and Use Committee before the commencement of any experiments.

Serum biochemistries.—Blood was collected before *in vivo* baseline and endpoint scans using tail vein collection. Blood was spun down for 10 minutes in a centrifuge (LW Scientific Combo M24 Centrifuge, Lawrenceville, GA, USA) at ~12,000 RPM to collect approximately 200μL of serum for biochemistry assays. Serum was used for analysis of blood urea nitrogen (BUN) by colormetric assay (BioAssay Systems) and intact parathyroid hormone (iPTH) by ELISA (Immunotopics).

In-vivo Micro-Computed Tomography of the distal tibia.—Under isoflurane anaesthesia, rats were placed supine in the bed of the Skyscan 1176 μCT (Bruker, Billerica, MA, USA). Right distal tibias were secured in a polystyrene holder with the tail and contralateral foot adjusted to be outside the field of view to assure clear isolation of the right distal tibia as previously described [28]. All scans were performed at 9μm voxel resolution, 1mm Al filter, 0.5° rotation step, and no frame averaging. Each scan lasted approximately 10 minutes.

The μCT scans for each animal were first manually registered in manufacturer supplied software (DataViewer version 1.5.2.4, Bruker) to align the scans, followed by a computerized approach using a pseudo 3D registration strategy, 50 (pixel) shift range, and a rotation range of 25 in degree. Registered images were used to define three volume of interests (VOIs) located at 4mm, 4.5mm, and 5mm's distal to the tibia-fibular junction (TFJ) to measure cortical porosity using manufacturer supplies software (CTAn version 1.14.3, Bruker). Each VOI was comprised of 5 consecutive slices. For each slice, the cortical bone was isolated using a hand drawn ROI to demarcate the endocortical and periosteal surfaces. These images of isolated cortical bone were processed further using MATLAB.

Custom MATLAB code tracking individual pore tracking.—All CT images, across all animals and VOIs, were imported into a custom MATLAB (Matrix Laboratory, MathWorks) script designed to track pores over time through a coordinate based (x, y, and z) identifying system. The script first defines an optimal threshold (using the Otsu method) across all animals and slices to use for segmentation of bone from void. A pore was defined as an area with more than 5 connected pixels in 2D space (486 um^2) so as to exclude background noise and vascular channels. To match pores in repeat scans, the script indexed each pore via a spatial grid allowed for pixel matching and relationship determination. Pores were indexed based on whether they existed just in the baseline image, both baseline and endpoint images, or just endpoint images. Pore relationships were established by determining which pores shared pixels. Four basic pore relationships were determined to capture some basic dynamic pore activities:

1. developed - present in endpoint image, but not in baseline image
2. expanded - present in both baseline and endpoint images, but the pore is larger at endpoint than at baseline
3. filled – present in baseline image, not in endpoint image
4. contracted – present in both baseline and endpoint images, but the pore is smaller at endpoint than at baseline

The pores were captured as changing dynamic entities when the net change in pixel size was greater than 1 pixel. This permitted the designation into appropriate pore category. If a pore was unchanged from baseline to endpoint it was considered 'static'. For each animal, data is presented as cumulative totals.

Statistics.—Data from baseline and endpoint measures were compared using a paired t-test with statistical difference defined as $p<0.05$. All statistical analyses were completed with SPSS Statistics 26 (IBM). Data are represented as mean ± standard deviation.

RESULTS

Experiment 1

Serum blood urea nitrogen was elevated in adenine mice indicating the presence of kidney disease.—At 10 weeks, BUN was higher in adenine vs. control ($p<0.0001$). At 14 weeks, there was a main effect of disease ($p<0.0001$), Ca-H_2O ($p=0.001$), and a disease-by-Ca-H_2O interaction ($p<0.0001$). All adenine groups had higher BUN than control groups. Ca-H_2O increasing BUN in adenine groups compared to untreated adenine. Both Con+1.5% and Con+3% groups had lower BUN than untreated control (Figure 2a). Kidney crystals were present, but they were not different across adenine groups at the 14-week time point ($p=0.143$; Figure 2b).

Serum PTH was higher in adenine mice at 10 and 14 weeks while Ca-H_2O suppressed PTH in 14-week adenine mice.—At 10 weeks, PTH was higher in adenine vs. control ($p=0.002$). At 14 weeks, there was a main effect of disease ($p=0.034$), a main effect of Ca-H_2O ($p<0.0001$), and a disease-by-Ca-H_2O interaction ($p=0.003$). At the 14-week timepoint, the untreated adenine group had higher PTH than all other groups with the Ad+1.5% and Ad+3% groups not statistically different from any of the control groups (Figure 3a).

Ca-H_2O resulted in lower cortical porosity in adenine mice after 4 weeks of treatment.—At 10 weeks, adenine mice had no differences in cortical area ($p=0.601$), but lower cortical thickness versus controls ($p<0.0001$). At this time point, cortical porosity was also higher in adenine mice vs control ($p<0.0001$; Figure 3b). Pore number was also higher in adenine mice compared to controls ($p<0.0001$; Table 1). At 14 weeks, there was no effect on cortical area ($p=0.324$), but there was statistical differences in cortical thickness ($p<0.0001$) with a main effect of disease ($p<0.0001$) and a main effect of Ca-H_2O ($p=0.001$), but no interaction effect ($p=0.594$). Cortical thickness was lowest in untreated adenine mice followed by adenine mice with calcium water supplementation with Ca-H_2O-treated control mice having the highest cortical thickness (Table 1). For cortical porosity at 14-weeks, there was a main effect of disease ($p<0.0001$), a main effect of Ca-H_2O ($p<0.0001$), and a disease-by-Ca-H_2O interaction ($p<0.0001$). At the 14-week timepoint, the untreated adenine group had higher porosity than all other groups. Calcium-treated adenine mice had porosity values not different from control mice (Figure 3b; Figure 3c). Additionally, there was a main effect of disease, a main effect of Ca-H_2O, and an interaction effect on pore number at 14-weeks

(p<0.0001 for all). Pore number was highest in untreated adenine with Ad+1.5% lower than untreated adenine and Ad+3% not different from any of the control groups (Table 1).

Ca-H_2O improved ultimate force in adenine-induced CKD mice compared to untreated adenine mice.—At 10 weeks, adenine mice had lower ultimate force compared to control mice (p=0.009; Table 1) however, post-yield displacement (p=0.618), stiffness (p=0.05), total work (p=0.085), and toughness (p=0.614) were not statistically different (Table 1). At 14 weeks, untreated adenine mice exhibited the lowest ultimate force of all groups with a main effect of disease (p=0.008) while Ca-H_2O led to higher ultimate force in both control and adenine-treated mice (main effect of Ca-H_2O p=0.001; Table 1); however, there was no interaction effect (p=0.127). Post-yield displacement was not different between all groups regardless of treatment at 14 weeks (p=0.426). Stiffness showed a disease-by-Ca-H_2O interaction effect (p=0.003). All adenine groups displayed lower stiffness compared to Con+3%, with a main effect of disease (p<0.0001). Ca-H_2O had no main effect on stiffness (p=0.103) despite the Con+3% group having the highest stiffness. Stiffness was not different between all adenine groups. At 14 weeks, all control groups had higher total work compared to untreated adenine mice with a main effect of disease (p=0.006), but no disease-by-Ca-H_2O interaction effect (p=0.096) or main effect of Ca-H_2O (p=0.893). Toughness was not different between all groups regardless of disease or treatment at 14 weeks (p=0.425) (Table 1).

Experiment 2

Ca-H_2O suppresses PTH without altering BUN.—During the 5-week treatment phase, BUN in Cy/+ rats was not different from baseline to endpoint (p=0.149; Figure 4a). At baseline all rats had PTH values ranging between 500-2500 pg/mL, but following Ca-H_2O, PTH values ranged between ~30-80 pg/mL (p=0.012; Figure 4b).

Cortical porosity decreases after a 5-week period of Ca-H_2O due to individual pore infilling.—Cortical porosity in distal tibia of the 6 animals at baseline ranged between 0.5% to 10.1%, illustrating the heterogeneity of disease within the model (Figure 5a and 5b). After 5 weeks of Ca-H_2O, cortical porosity was less than 1% in all animals (p=0.163; Figure 5a). Individual pore tracking demonstrated that the predominate pore action during the 5-week treatment period was complete pore infilling (85%), while 12% of pores got smaller (contracted), and 3% of pores were newly developed; no pores were quantified as getting larger (expanding) and only one pore was static (no change in pore size) from baseline to endpoint (Figure 5c).

DISCUSSION

Utilizing two animal models of CKD, our studies demonstrate that cortical porosity is reduced after suppression of PTH via calcium water supplementation. Additionally, we were able to track individual pores over time, demonstrating that PTH suppression resulted in pore infilling and prevention of new pore formation. Notably, we allowed cortical pores to develop in both of our models prior to the initiation of treatment unlike previous studies that utilized calcium water supplementation to prevent pore formation by initiating treatment in

the early stages of the disease progression [15] [14]. Overall, these data show that cortical pore reduction/infilling is possible in animal models of CKD. This research creates a foundation for future research to test and explore clinically relevant therapies in a CKD population which may also have the potential to cause net pore infilling.

Adenine-induced CKD and the Cy/+ rat model are both clinically relevant as they model the human characteristics of CKD-MBD with the progressive development of elevated PTH and cortical porosity. Utilizing the high resolution of HR-pQCT scans, Nickolas, *et al.,* quantified the rapid development of cortical porosity averaged per year in CKD patients and found cortical deterioration was predicted by serum PTH [13]. In both the Cy/+ rat and adenine-induced CKD in mice, we have demonstrated progressive development of cortical porosity over time and that the highest levels of cortical porosity are concurrent with high PTH [21] [28]. It is important to note that the structure of the cortical bone varies between rodents and humans due to the lack of osteons in rodents; however, cortical porosity develops in both humans and rodents indicating the potential for similar mechanisms despite structural differences.

In both preclinical and clinical settings, little is known about the development of cortical porosity in CKD other than correlations with PTH. We have previously seen that rodents (Cy/+ rat) placed on calcium water supplementation prior to the development of cortical porosity never form pores [15] [14] likely demonstrating the importance of PTH in the development of porosity. While little is known about the mechanisms that lead to the development of cortical pores in CKD, even less is known about what happens to those pores once they form and if porosity can be reversed.

In adenine-induced CKD mice, cortical porosity measured at the distal 1/3 femur was 2.7-3.1% at both 10 weeks and 14 weeks after the initiation of the adenine diet (Fig. 3b). At 14 weeks, after 4 weeks of either 1.5% or 3% calcium water supplementation, cortical porosity was 0.3-0.8%, approximately a 70-90% reduction compared to the levels in untreated animals (Fig. 3b). *In vivo* longitudinal scans of Cy/+ rats showed similar effects on cortical porosity at the distal tibia after calcium water supplementation, with porosity of animals averaging 3.1% prior to treatment and 0.5% after calcium water supplementation. Given that we tracked pores longitudinally within the same animal we can conclude that cortical pores infilled and new pore formation/expansion was suppressed. In both animal models, the reduction in cortical porosity coincided with suppression of PTH. These studies demonstrate that cortical pore reversal is possible in rodent models. Further research is required to understand if or to what degree cortical pores in human bone can infill.

The presence of cortical porosity is associated with reductions in bone mechanical properties in preclinical models [14] [15] and in human bone samples [29] as well as associations with fracture in clinical studies [30] [31] [32] [33]. Thus, the goal of pore infilling would be to normalize mechanical properties and reduce fracture risk. After 14 weeks of adenine-induced CKD, untreated adenine mice had 11% lower ultimate force versus untreated controls. Compared with aged-matched untreated adenine mice, groups treated with calcium water supplementation for 4 weeks had 70-90% lower cortical porosity and 14-18% higher ultimate force. It is important to note that our porosity measures were in the distal third of

the femur while our mechanical assessment was at the midshaft thus we cannot directly conclude the effects were mediated by porosity. Calcium-water supplementation also resulted in higher cortical thickness in treated adenine mice vs. untreated adenine mice which likely also contributes to improved mechanical properties. Given the fact that matrix properties are often compromised in CKD, the absence of complete normalization of mechanical properties is not a complete surprise – yet the fact that there is a beneficial effect on bone strength is encouraging. Additionally, we cannot completely determine if this is an effect of having fewer cortical pores or is an independent effect of calcium water supplementation since control calcium water-treated mice also had some increases in ultimate force. However, our results show that 1.5% calcium supplementation has minimal effect on ultimate force on control mice (0.4% higher vs. untreated controls) whereas, adenine mice on the same treatment demonstrated greater increases on ultimate force (18% higher vs. untreated adenine). We hypothesize the large differences between adenine and control groups with 1.5% calcium water supplementation is due to pore reduction. Future work will need to further address the impact of pore reversal on mechanical properties of bone.

Longitudinal cortical porosity has been previously measured in both human studies and animal models [13] [28]; yet, studies investigating the dynamics of individual pores over time are lacking. Cortical porosity measures over time could be affected in many ways that are not necessarily reflected if total porosity is the only variable assessed. For example, one large pore could fill in modestly while multiple new smaller pores may form, leaving overall porosity unchanged; yet, it is unknown how these differences in the size and number of pores may impact overall mechanical properties. Our approach in Experiment 2 with the Cy/+ rat model, provides a unique insight into individual cortical pore dynamics. Unlike cortical porosity that only quantifies porosity within a given VOI or slice, our approach of individual pore tracking permits us to measure the change of each pore, individually, over time. This showed, for example, that in the Cy/+ rat with the highest porosity at baseline (10.1%), most pores filled in after treatment, yet a small number of pores also developed (Figure 5C). This technological approach to individual pore tracking has the potential to better inform dynamics of cortical porosity over time using CT in both pre-clinical and perhaps clinical studies.

These results provide proof-of-concept data about pore infilling – the first of many steps. Further research will be required to determine whether the effects of cortical pore reduction and pore infilling as seen in this study stimulated by calcium water supplementation is a result of extra exogenous calcium in the circulation, suppression of PTH, or a combination of exogenous calcium and PTH suppression. Furthermore, calcium water supplementation is not a clinically viable treatment since CKD patients are already at an increased risk of extracellular and vascular calcification. In our current study with mice, BUN was higher in adenine mice with calcium water supplementation which could allude to worsening of kidney disease in this model as well. Despite the treatment method of calcium water being a clear limitation for clinical translatability, this study presents unique longitudinal data showing the refilling of individual pores which is has conceptual novelty. Therefore, future studies must examine whether PTH suppression is critical for cortical pore infilling to occur

as well as discover what clinically relevant therapies are available that can stimulate pore infilling.

The tissue-level mechanisms underlying pore formation and infilling in the context of CKD are largely unknown. Pores can be stimulated in rodent models via administration of PTH [34] and in female rats fed a low calcium diet during lactation [35] [36]. In lactation models, there is evidence of bone formation on pore surfaces [36]. While the dynamic nature of osteoclast and osteoblast activity on pore surfaces in rodents is sometimes called intra-cortical remodeling [35] [36], it is critical to differentiate this from intra-cortical remodeling in larger mammals within the more normal primary/secondary osteonal structure of cortical bone. In rodents, remodeling does not occur within the cortex under normal physiological conditions. Nonetheless, it is noteworthy that both rodents and humans develop cortical porosity in CKD which indicates the mechanisms potentially may not be linked to physiological intra-cortical remodeling. In other conditions, like aging, cortical porosity develops due to intracortical remodeling in both rodents and humans [37] [38]. This further demonstrates that differences in cortical bone structure may not preclude animal models from having value for studying mechanisms of cortical porosity development and infilling. Further research will need to address the mechanism inducing pore infilling in rodents.

Limitations of our two experiments include the use of only male Cy/+ rats and only female adenine mice. While sex differences in cortical pore dynamics are of interest for future work, our use of a single sex in each study together still demonstrate that reduction/infilling of cortical pores occurs with calcium water supplementation in two progressive models of CKD. Furthermore, we were prevented from doing longitudinal pore tracking in mice due to the limitations of resolution of *in vivo* μCT relative to pore sizes in mice. We are not able to directly determine if cortical porosity was responsible for the mechanical benefit in the mouse study as our assessment of porosity was not directly at the site of testing. Additionally, as mentioned above, our use of calcium water supplementation is of itself not clinically relevant, however, as a suppressor of PTH, it provides a proof-of-concept that cortical pores can infill. Future studies will also need to address the mechanisms of cortical pore infilling utilizing techniques like dynamic histomorphometry to track formation over time within pores. Finally, there was a pattern of difference between 10 and 14 week adenine mice that hint at reduced BUN at the later timepoint. If kidney function improved over time this would complicate the interpretation of the model, although it is noted that both porosity and PTH remain well above normal at the 14 week timepoint.

In conclusion, our work demonstrates that cortical pores that develop in the setting of CKD are capable of infilling in rodent models. Future work should focus on what therapies are best suited to stimulate pore infilling and whether this is possible in humans. Ideally, determining the best therapeutic strategy to both infill existing pores as well as prevent new pores from developing may provide the best scenario to improve bone health in CKD patients through the reduction in skeletal fragility.

Acknowledgements

This work was supported by NIH DK110871, DK110429 and VA Merit awards I01BX001471 and I01BX003025.

References

[1]. Alem AM et al., "Increased risk of hip fracture among patients with end-stage renal disease," Kidney Int., vol. 58, no. 1, pp. 396–399, 2000. [PubMed: 10886587]

[2]. Moe SM and Nickolas TL, "Fractures in Patients with CKD: Time for Action," Clin. J. Am. Soc. Nephrol, vol. 11, no. 11, pp. 1929–1931, 2016. [PubMed: 27797903]

[3]. Maravic M, Ostertag A, Torres PU, and Cohen-Solal M, "Incidence and risk factors for hip fractures in dialysis patients," Osteoporos. Int, vol. 25, no. 1, pp. 159–165, 2014. [PubMed: 23835863]

[4]. Kuo CH et al., "Increased risks of mortality and atherosclerotic complications in incident hemodialysis patients subsequently with bone fractures: A nationwide case-matched cohort study," PLoS One, vol. 10, no. 4, pp. 1–13, 2015.

[5]. Kim SM, Long J, Montez-Rath M, Leonard M, and Chertow GM, "Hip Fracture in Patients With Non-Dialysis-Requiring Chronic Kidney Disease," J. Bone Miner. Res, vol. 31, no. 10, pp. 1803–1809, 2016. [PubMed: 27145189]

[6]. Tentori F et al., "High rates of death and hospitalization follow bone fracture among hemodialysis patients," Kidney Int., vol. 85, no. 1, pp. 166–173, 2014. [PubMed: 23903367]

[7]. Coco M and Rush H, "Increased incidence of hip fractures in dialysis patients with low serum parathyroid hormone," Am. J. Kidney Dis, vol. 36, no. 6, pp. 1115–1121, 2000. [PubMed: 11096034]

[8]. C. for D. C. and Prevention, "Chronic Kidney Disease in the United States, 2019," Atlanta, GA US Dep. Heal. Hum. Serv. Centers Dis. Control Prev, 2019.

[9]. Nickolas TL, Leonard MB, and Shane E, "Chronic kidney disease and bone fracture: A growing concern," Kidney Int., vol. 74, no. 6, pp. 721–731, 2008. [PubMed: 18563052]

[10]. Ketteler M et al., "Diagnosis, evaluation, prevention, and treatment of chronic kidney disease-mineral and bone disorder: Synopsis of the kidney disease: Improving global outcomes 2017 clinical practice guideline update," Ann. Intern. Med, vol. 168, no. 6, pp. 422–430, 2018. [PubMed: 29459980]

[11]. Miller PD, "Chronic kidney disease and the skeleton," Bone Res., vol. 2, 2015.

[12]. Parfitt AM, "Perspective: A structural approach to renal bone disease," J. Bone Miner. Res, vol. 13, no. 8, pp. 1213–1220, 1998. [PubMed: 9718188]

[13]. Nickolas TL et al., "Rapid cortical bone loss in patients with chronic kidney disease," J. Bone Miner. Res, vol. 28, no. 8, pp. 1811–1820, 2013. [PubMed: 23456850]

[14]. Moe SM et al., "Anti-sclerostin antibody treatment in a rat model of progressive renal osteodystrophy," J. Bone Miner. Res, vol. 30, no. 3, pp. 539–549, 2015.

[15]. Moe SM et al., "A comparison of calcium to zoledronic acid for improvement of cortical bone in an animal model of CKD," J. Bone Miner. Res, vol. 29, no. 4, pp. 902–910, 2014. [PubMed: 24038306]

[16]. Moe SM et al., "A rat model of chronic kidney disease-mineral bone disorder," Kidney Int., vol. 75, no. 2, pp. 176–184, 2009. [PubMed: 18800026]

[17]. Newman CL et al., "Cortical bone mechanical properties are altered in an animal model of progressive chronic kidney disease," PLoS One, vol. 9, no. 6, pp. 1–8, 2014.

[18]. Jia T et al., "A novel model of adenine-induced tubulointerstitial nephropathy in mice - 1471-2369-14-116.pdf," 2013.

[19]. Tani T, Orimo H, Shimizu A, and Tsuruoka S, "Development of a novel chronic kidney disease mouse model to evaluate the progression of hyperphosphatemia and associated mineral bone disease," Sci. Rep, vol. 7, no. 1, pp. 1–12, 2017. [PubMed: 28127051]

[20]. Santana AC et al., "Thalidomide suppresses inflammation in adenine-induced CKD with uraemia in mice," Nephrol. Dial. Transplant, vol. 28, no. 5, pp. 1140–1149, 2013. [PubMed: 23345625]

[21]. Metzger CE, Swallow EA, and Allen MR, "Elevations in Cortical Porosity Occur Prior to Significant Rise in Serum Parathyroid Hormone in Young Female Mice with Adenine - Induced CKD," Calcif. Tissue Int, 2019.

[22]. Katsumata K et al., “Sevelamer hydrochloride prevents ectopic calcification and renal osteodystrophy in chronic renal failure rats,” Kidney Int., vol. 64, no. 2, pp. 441–450, 2003. [PubMed: 12846739]

[23]. Neven E, Dauwe S, De Broe ME, D’Haese PC, and Persy V, “Endochondral bone formation is involved in media calcification in rats and in men,” Kidney Int., vol. 72, no. 5, pp. 574–581, 2007. [PubMed: 17538568]

[24]. Neven E et al., “Adequate phosphate binding with lanthanum carbonate attenuates arterial calcification in chronic renal failure rats,” Nephrol. Dial. Transplant, vol. 24, no. 6, pp. 1790–1799, 2009. [PubMed: 19144999]

[25]. Ferrari GO et al., “Mineral bone disorder in chronic kidney disease: Head-to-head comparison of the 5/6 nephrectomy and adenine models,” BMC Nephrol., vol. 15, no. 1, pp. 1–7, 2014. [PubMed: 24386889]

[26]. Allen MR, Newman CL, Chen N, Granke M, Nyman JS, and Moe SM, “Changes in skeletal collagen cross-links and matrix hydration in high- and low-turnover chronic kidney disease,” Osteoporos. Int, vol. 26, no. 3, pp. 977–985, 2015. [PubMed: 25466530]

[27]. Allen MR et al., “Skeletal effects of zoledronic acid in an animal model of chronic kidney disease,” Osteoporos. Int, vol. 24, no. 4, pp. 1471–1481, 2013. [PubMed: 22907737]

[28]. Mcnerny EMB, Buening DT, Aref MW, Chen NX, Moe SM, and Allen MR, “Time course of rapid bone loss and cortical porosity formation observed by longitudinal μCT in a rat model of CKD,” Bone, vol. 125, no. 4, pp. 16–24, 2019. [PubMed: 31059864]

[29]. Boughton OR et al., “Computed tomography porosity and spherical indentation for determining cortical bone millimetre-scale mechanical properties,” Sci. Rep, vol. 9, no. 1, pp. 1–15, 2019. [PubMed: 30626917]

[30]. Bala Y et al., “Cortical porosity identifies women with osteopenia at increased risk for forearm fractures,” J. Bone Miner. Res, vol. 29, no. 6, pp. 1356–1362, 2014. [PubMed: 24519558]

[31]. Bjørnerem Å, “The clinical contribution of cortical porosity to fragility fractures,” Bonekey Rep., vol. 5, no. October, pp. 1–5, 2016.

[32]. Krai R, Osima M, Borgen TT, Vestgaard R, Richardsen E, and Bjørnerem Å, “Increased cortical porosity and reduced cortical thickness of the proximal femur are associated with nonvertebral fracture independent of Fracture Risk Assessment Tool and Garvan estimates in postmenopausal women,” PLoS One, vol. 12, no. 9, pp. 1–15, 2017.

[33]. Sundh D, Mellstrom D, Nilsson M, Karlsson M, Ohlsson C, and Lorentzon M, “Increased cortical porosity in older men with fracture,” J. Bone Miner. Res, vol. 30, no. 9, pp. 1692–1700, 2015. [PubMed: 25777580]

[34]. Lotinun S et al., “Continuous parathyroid hormone induces cortical porosity in the rat: Effects on bone turnover and mechanical properties,” J. Bone Miner. Res, vol. 19, no. 7, pp. 1165–1171, 2004. [PubMed: 15177000]

[35]. Ruth E, “An experimental study of the Haversian-type vascular channels,” Anat. Rec, vol. 112, pp. 429–455, 1953.

[36]. Ross R and Sumner D, “Bone matrix maturation in a rat model of intra-cortical bone remodeling,” Calcif. Tissue Int, vol. 101, no. 2, pp. 193–203, 2017. [PubMed: 28374176]

[37]. Piemontese M et al., “Old age causes de novo intracortical bone remodeling and porosity in mice,” JCI insight, vol. 2, no. 17, pp. 1–18, 2017.

[38]. Nicks KM, Amin S, Atkinson EJ, Riggs BL, Melton LJ, and Khosla S, “Relationship of age to bone microstructure independent of areal bone mineral density,” J. Bone Miner. Res, vol. 27, no. 3, pp. 637–644, 2012. [PubMed: 22095490]

HIGHLIGHTS

- CKD-induced cortical porosity was reduced in rodent models after PTH suppression.
- Reducing cortical porosity improves bone mechanics in mice with CKD.
- Individual pore tracking over time documents pore infilling in CKD animals.

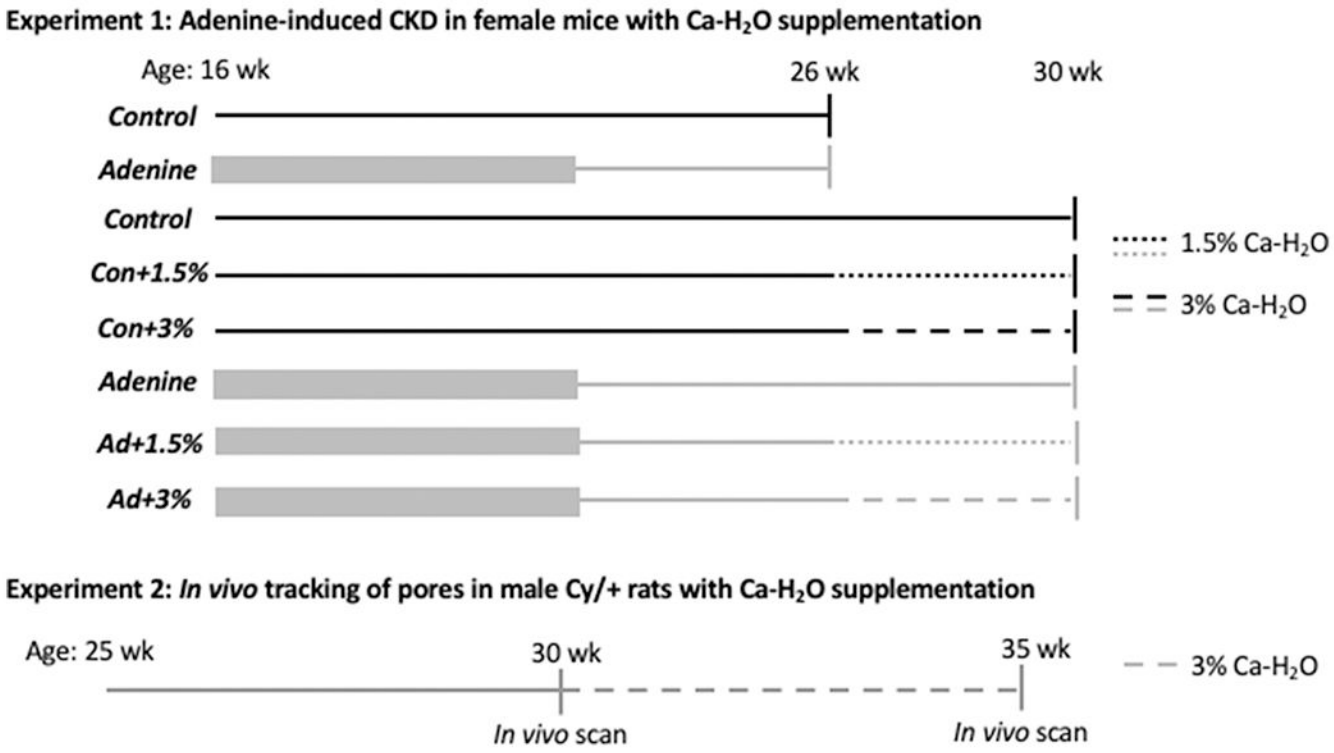

Figure 1.

Experimental design for experiment 1 (adenine-induced CKD in mice) and experiment 2 (Cy/+ rat). Black lines represent Control groups while and grey lines represent CKD (Exp 1 = adenine, Exp 2 = Cy/+). Thick grey lines indicate induction period of 0.2% adenine diet in adenine-induced CKD mice. Thin lines represent times on control diet. Solid lines represent untreated periods and dashed lines are periods treated with calcium water supplementation (1.5% or 3%).

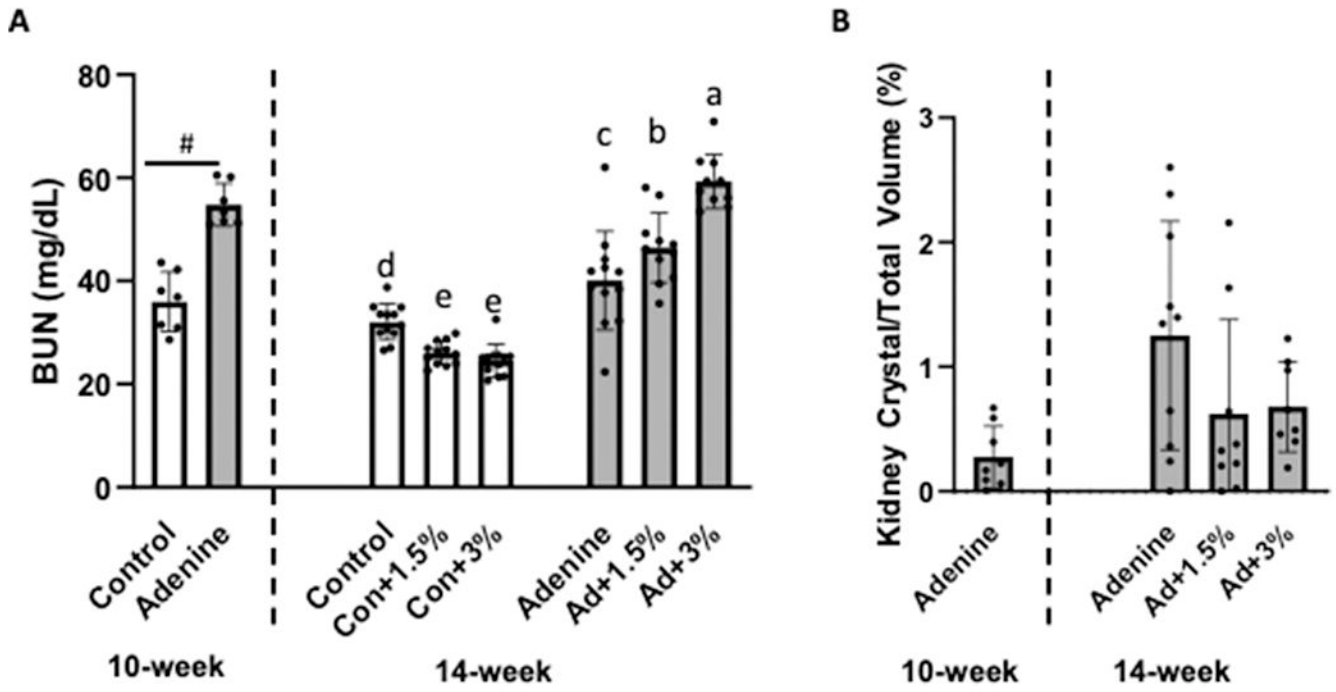

Figure 2.

Serum blood urea nitrogen (BUN) and kidney crystal assessment in adenine-induced CKD mice (n=10-12/group). A) Serum BUN was higher in adenine vs. control at 10 weeks. At 14 weeks, serum BUN was lower in both Con+1.5% and Con+3% compared to untreated Con while Ca-H_2O supplementation increased BUN in adenine groups. [#]Indicates statistical difference in t-test at 10 weeks. At 14 weeks, bars not sharing the same letter are statistically different. B) Kidney crystals were present in adenine mice with no statistical differences due to Ca-H_2O treatment.

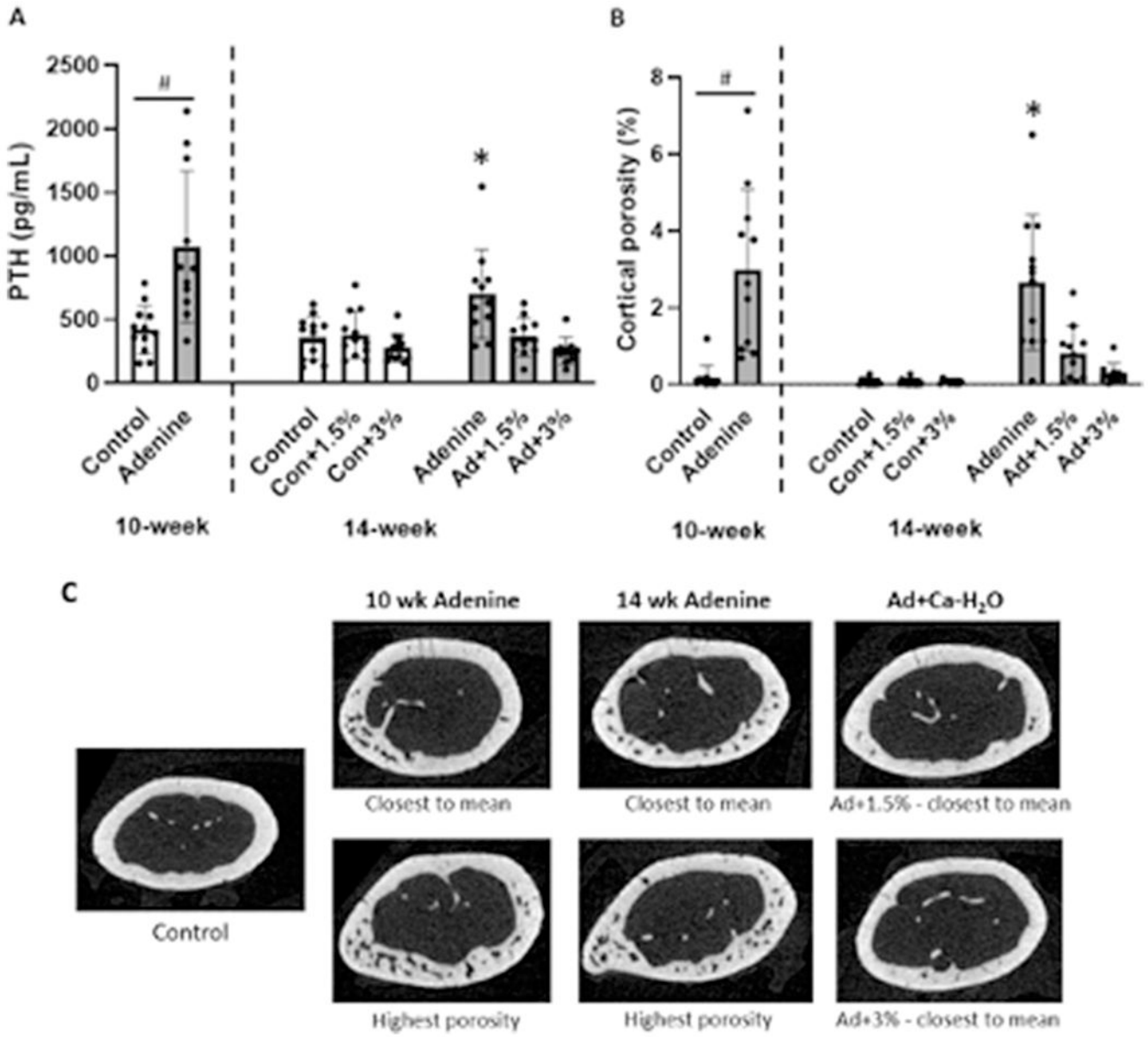

Figure 3.

Serum parathyroid hormone (PTH) and cortical porosity at the distal 1/3 femur in adenine-induced CKD mice (n=10-12/group). A) Serum PTH was higher in adenine mice at 10 weeks. At 14 weeks, the untreated adenine group had higher PTH than all other groups. #Indicates difference in t-test at 10 weeks ($p<0.05$). *Indicates statistically different from all other 14-week groups ($p<0.05$). B) At 10 weeks, cortical porosity was higher in adenine vs. control mice. At 14 weeks, the untreated adenine group had higher cortical porosity than Ca-H_2O-treated adenine groups and all control groups. #Indicates difference in t-test at 10 weeks ($p<0.05$). *Indicates statistically different from all other 14-week groups ($p<0.05$). C) Representative images of cortical bone in control and adenine-induced CKD mice.

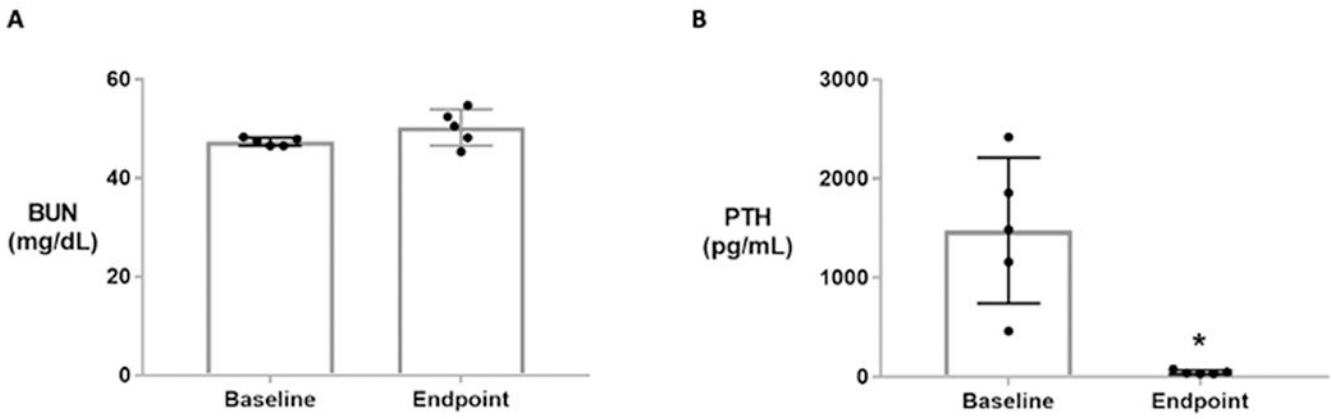

Figure 4.

Blood urea nitrogen (BUN) and parathyroid hormone (PTH) serum measures at baseline (30 weeks) and endpoint (35 weeks) in male Cy/+ rats (n=5). A) BUN is not different between baseline and endpoint. B) PTH significantly declined at endpoint due to 5 weeks of Ca-H2O treatment. * Indicates difference in a paired t-test ($p<0.05$).

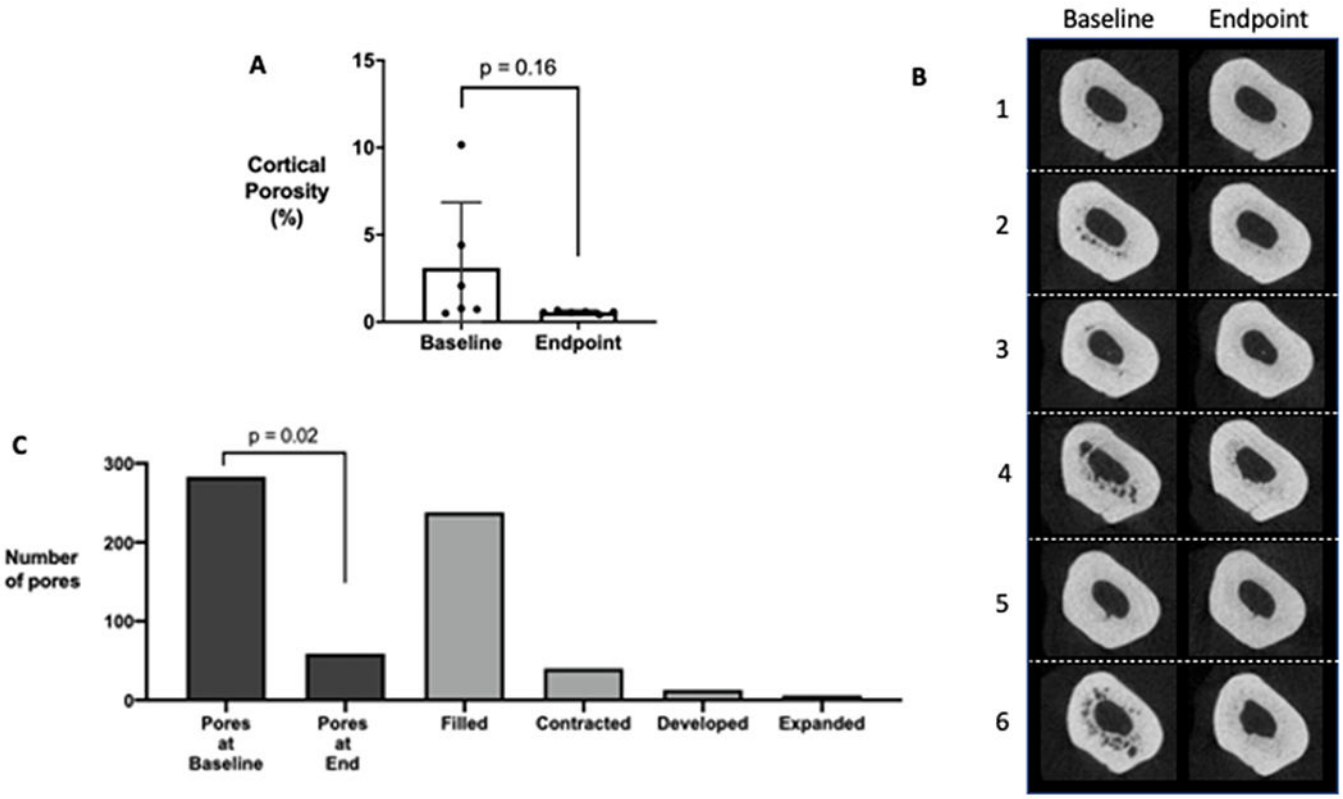

Figure 5.

Cortical porosity of the distal tibia before (baseline) and after (endpoint) calcium water supplementation via longitudinal *in vivo* μCT scans in male Cy/+ rats (n=6). (A) Quantification of cortical porosity with representative images shown in (B) for all animals used in the study. Note the heterogeneous development of cortical pores at baseline in this Cy/+ model with some CKD rats displaying low levels of cortical pores. There are no statistical differences in total porosity (repeated measures t-test analysis). (C) Individual pore tracking across all six animals quantified by the number of pores at baseline and endpoint as well as the number of pores completing a dynamic action (filled, contracted, developed, expanded). There were significantly less pores at the endpoint compared to baseline (repeated measures t-test analysis).

Table 1.

Cortical bone parameters measured from the distal 1/3 femur and mechanics properties from 3-pt-bend test of the contralateral femur of adenine-induced CKD mice. Group values not sharing the same superscript letters are statistically different ($p<0.05$ from a Student's t-test for 10-week values and from a Duncan post-hoc following a 2X3 ANOVA for 14-week data). Group values without letters have no statistical differences.

	Cortical Bone Area (mm^2)	Cortical Thickness (mm)	Pore Number ($\#/mm^2$)	Ultimate Force (N)	Postyield Displacement (μm)	Stiffness (N/mm)	Total Work (mJ)	Toughness (Mpa)
10-week								
Control	0.68 ± 0.06	0.14 ± 0.01^{a}	0.08 ± 0.1^{a}	18.10 ± 1.91^{a}	269 ± 142	75.28 ± 5.33	6.05 ± 1.82	2.20 ± 0.81
Adenine	0.69 ± 0.03	0.12 ± 0.01^{b}	1.06 ± 0.71^{b}	16.19 ± 2.26^{b}	242 ± 106	69.78 ± 7.27	4.89 ± 1.17	2.05 ± 0.53
14-week								
Control	0.69 ± 0.40	0.14 ± 0.01^{ab}	0.03 ± 0.04^{a}	17.92 ± 0.94^{b}	298 ± 19	82.37 ± 5.38^{ab}	6.26 ± 1.83^{a}	2.18 ± 0.70
Con +1.5%	0.70 ± 0.56	0.15 ± 0.01^{a}	0.03 ± 0.03^{a}	18.67 ± 2.21^{ab}	265 ± 190	82.34 ± 6.99^{ab}	5.78 ± 1.81^{a}	2.13 ± 0.44
Con+3%	0.74 ± 0.05	0.16 ± 0.01^{a}	0.04 ± 0.03^{a}	20.62 ± 1.80^{a}	180 ± 93	88.34 ± 7.83^{a}	5.78 ± 1.16^{a}	1.87 ± 0.38
Adenine	0.66 ± 0.09	0.11 ± 0.01^{d}	0.94 ± 0.58^{c}	15.83 ± 2.69^{c}	232 ± 196	74.71 ± 6.63^{b}	4.32 ± 1.54^{b}	1.77 ± 0.71
Ad+1.5%	0.65 ± 0.21	0.13 ± 0.03^{c}	0.33 ± 0.25^{b}	18.74 ± 3.46^{ab}	204 ± 53	78.63 ± 12.43^{b}	5.14 ± 0.79^{ab}	1.93 ± 0.42
Ad+3%	0.70 ± 0.07	0.13 ± 0.01^{bc}	0.17 ± 0.10^{ab}	18.10 ± 1.52^{b}	244 ± 74	79.75 ± 7.38^{b}	5.32 ± 1.24^{ab}	1.96 ± 0.35